

Gravity Waves over Terrain in High-Resolution Global MPAS Simulations

Joe Klemp, Bill Skamarock,
Michael Duda, Sang-Hun Park

National Center for Atmospheric Research



Based on unstructured centroidal Voronoi (hexagonal) meshes using C-grid staggering and selective grid refinement.

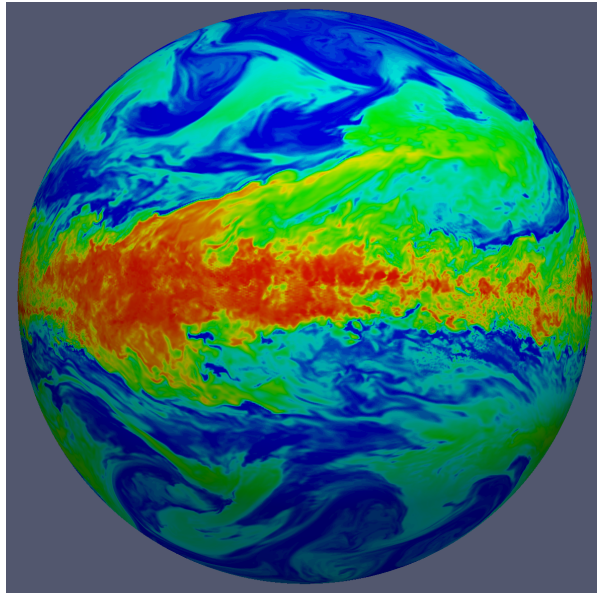
Jointly developed, primarily by NCAR and LANL/DOE

MPAS infrastructure - NCAR, LANL, others.

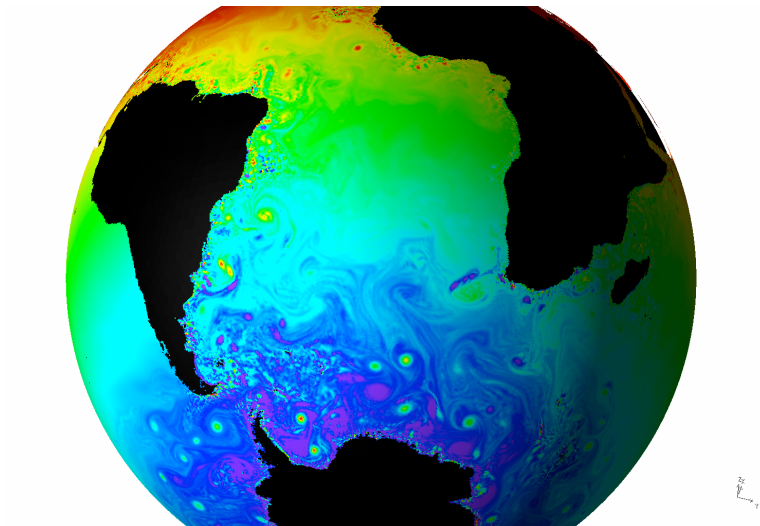
MPAS - Atmosphere (NCAR)

MPAS - Ocean (LANL)

MPAS - Ice, etc. (LANL and others)

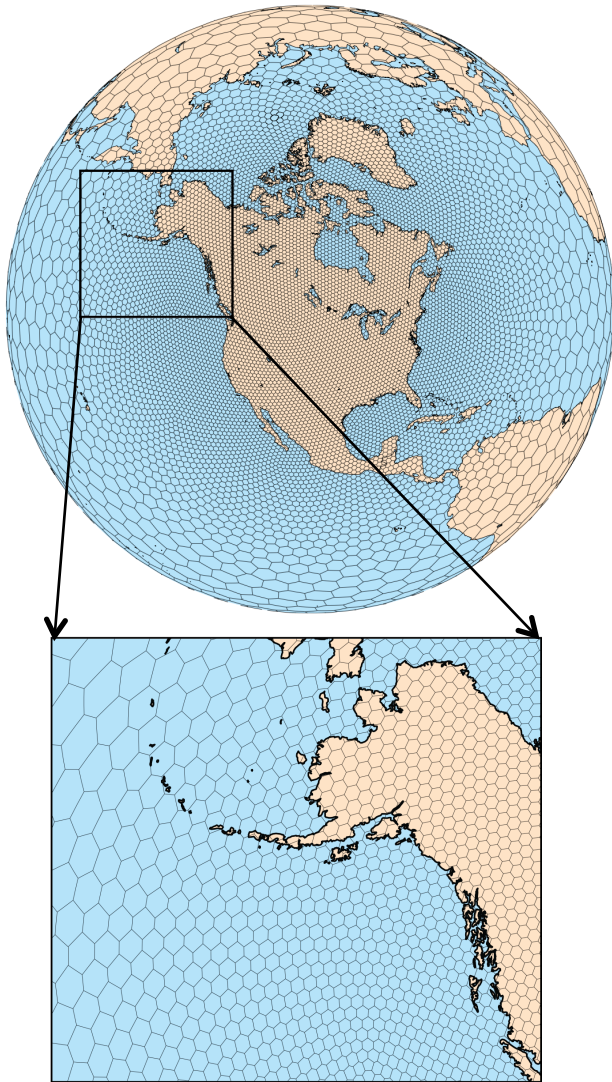


Atmosphere



Ocean

MPAS - Atmosphere



Applications

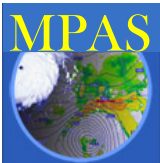
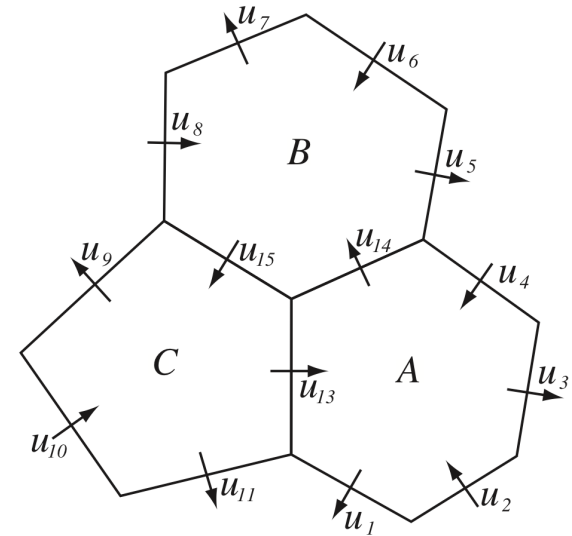
- NWP, Regional Climate and Climate

Equations

- Fully compressible nonhydrostatic equations
- Permits *explicit* simulation of clouds

Solver Technology

- C-grid centroidal Voronoi mesh
- Unstructured grid permits conformal variable-resolution grids
- Most of the techniques for integrating the nonhydrostatic equations come from WRF.
- ARW physics (Nested Regional Climate model configuration).



MPAS-A simulations on Yellowstone*

Global, uniform resolution.

| Ave. cell spacing | # Cell columns | Conv param |
|-------------------|----------------|------------|
| 60 km | 163,842 | yes |
| 30 km | 655,362 | yes |
| 15 km | 2,621,442 | yes, no |
| 7.5 km | 10,485,762 | yes, no |
| 3 km | 65,536,002 | no |

41 vertical levels, WRF-NRCM physics, prescribed SSTs.

Hindcast periods:

Baroclinic wave event: 23 October – 2 November 2010

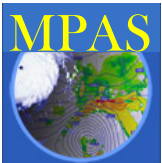
60, 30, 15, 7.5, 3 km meshes

Tropical cyclone events: 27 August – 6 September 2010

15 km, 3 km meshes

MJO event: 15 January – 4 February 2009

15 km, 7.5 km, 3 km meshes



* 1.5 petaflop IBM iDataPlex architecture with 72,288 processor cores

Implicit Rayleigh Absorbing Layer in Nonhydrostatic HEVI Time Integration Schemes

- Solve vertically implicit equation to obtain $w^{*\tau+\Delta\tau}$ and $\pi^{*\tau+\Delta\tau}$
- Apply implicit Rayleigh damping to $w^{*\tau+\Delta\tau}$:

$$w^{\tau+\Delta\tau} = w^{*\tau+\Delta\tau} - \Delta\tau R_w w^{*\tau+\Delta\tau}$$

- Adjust pressure to account for Rayleigh damping:

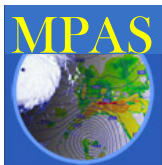
$$\pi^{\tau+\Delta\tau} = \pi^{*\tau+\Delta\tau} + f(w^{\tau+\Delta\tau} - w^{*\tau+\Delta\tau})$$

- Combining the intermediate steps, the w equation becomes:

$$\frac{\partial w}{\partial \tau} + c_p \theta^t \partial_z \overline{\pi'}^{\tau} - g \frac{\theta'^{\tau}}{\theta} + R_w w^{\tau+\Delta\tau} - \frac{\Delta\tau^2 c^2}{4\rho^t \theta^t} \frac{\partial}{\partial z^2} \left\{ \rho^t \theta^t R_w w^{\tau+\Delta\tau} \right\} = F_w^t$$

Normal Rayleigh damping
term that vanishes in
hydrostatic limit

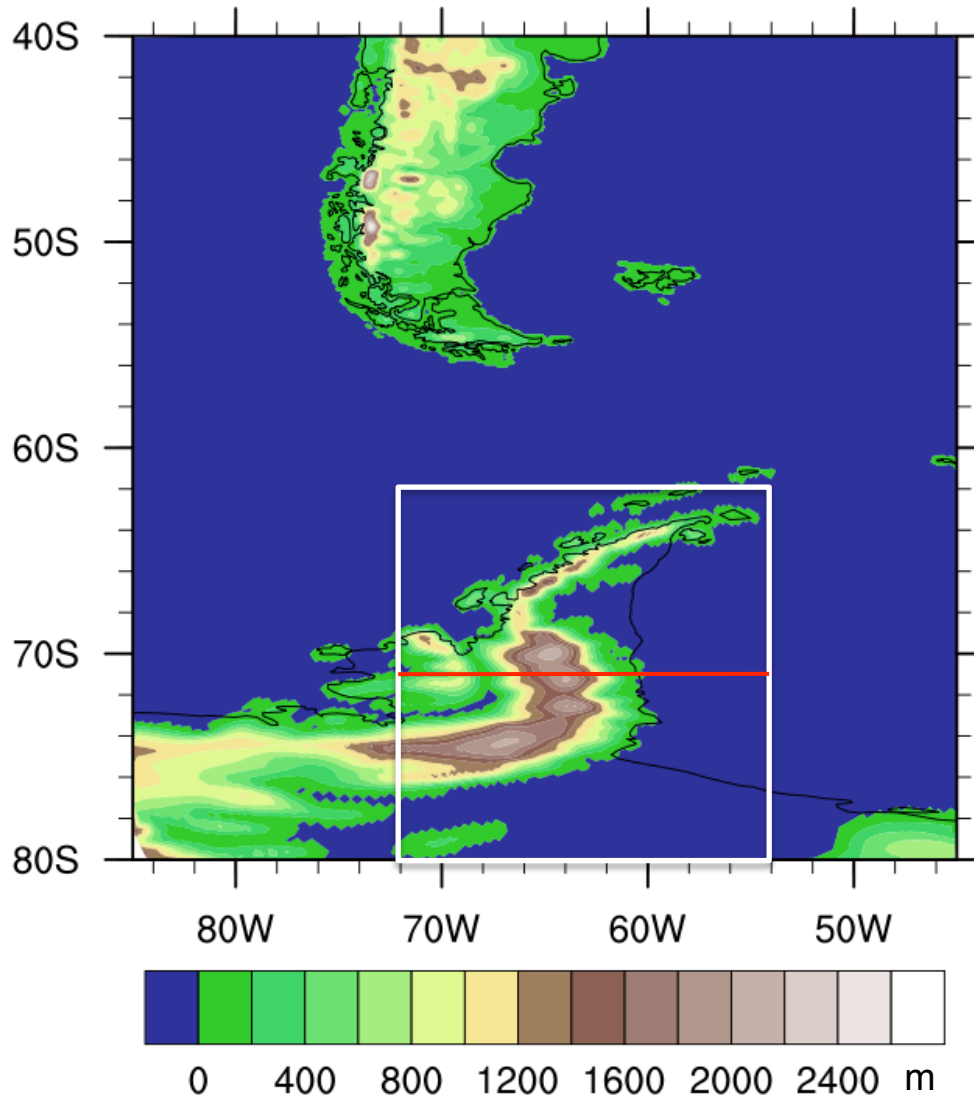
Additional damping term
that remains effective in
hydrostatic limit



Impact of Gravity Wave Absorbing Layer – Antarctic Peninsula

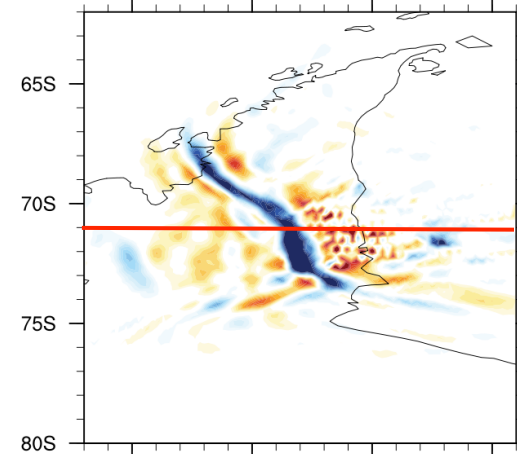
MPAS 2621442 Cell (15 km) 30 h Forecast, Valid 10-29-2010 06Z

Terrain



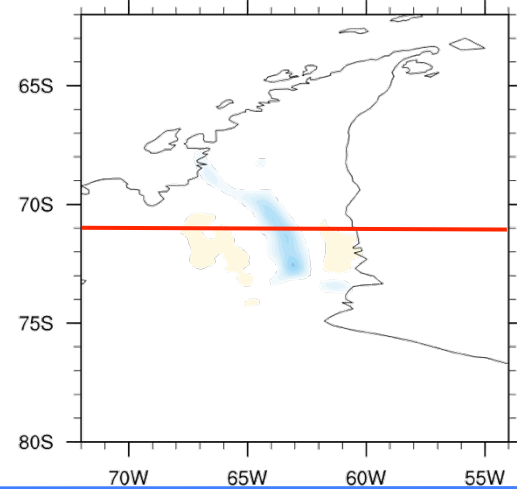
W at ~27 km without absorbing layer

w(m/s) at level-38 <-7.66085,7.59244>



W at ~27 km with absorbing layer

w(m/s) at level-38 <-2.09504,0.72404>

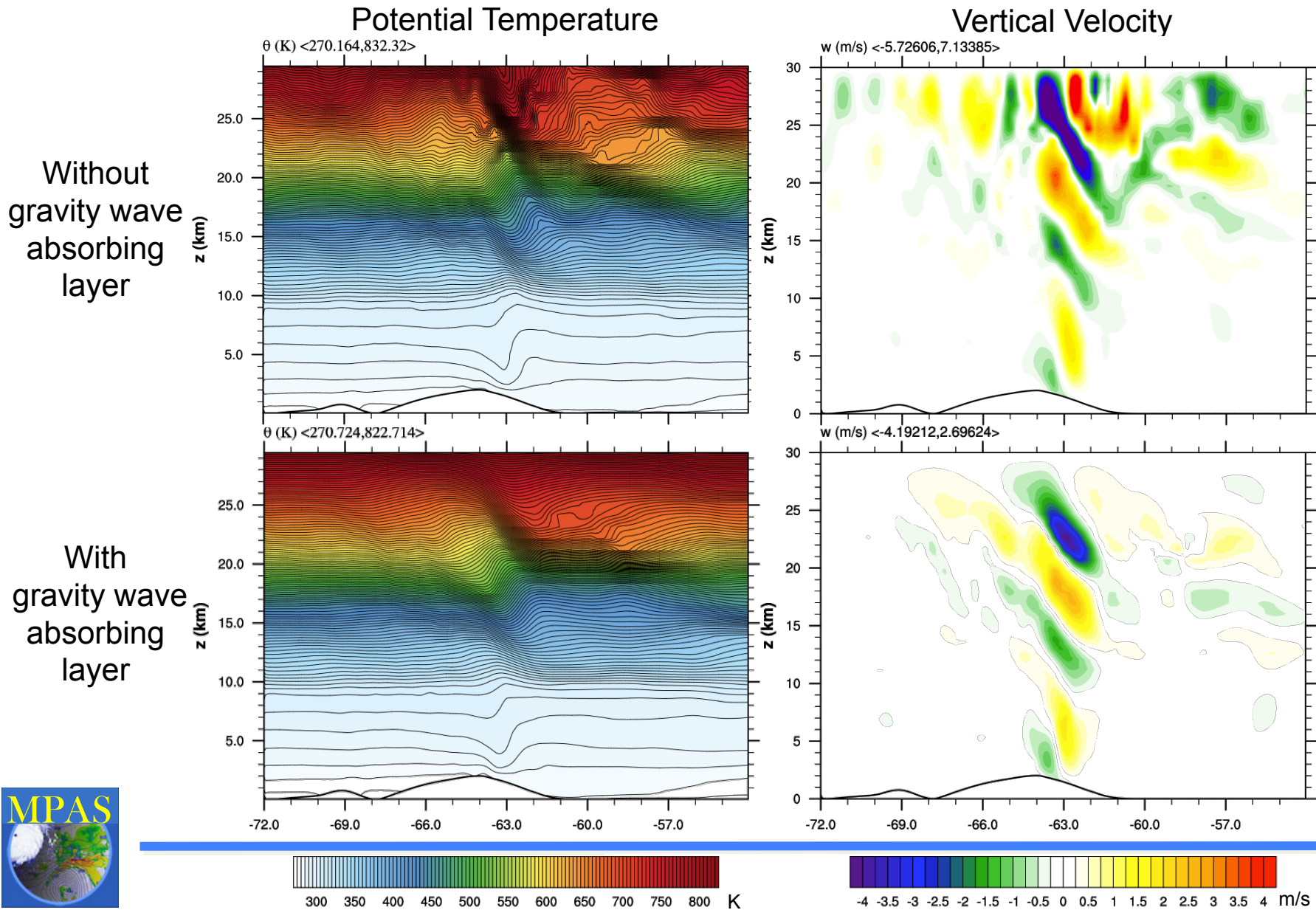


-4 -3 -2 -1 0 1 2 3 4 m/s



Impact of Gravity Wave Absorbing Layer – Antarctic Peninsula

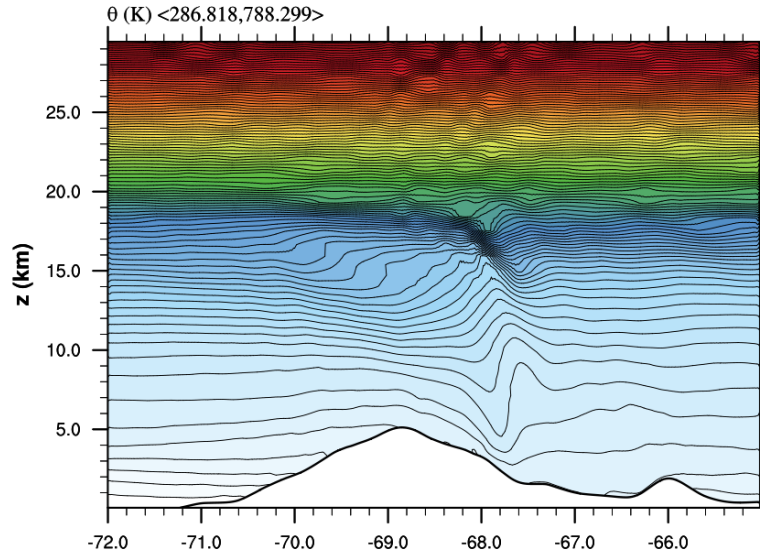
MPAS 30 h Forecast, Valid 10-29-2010 06Z, Cross sections at 71° S



Mountain Wave Dependence on Winds Aloft

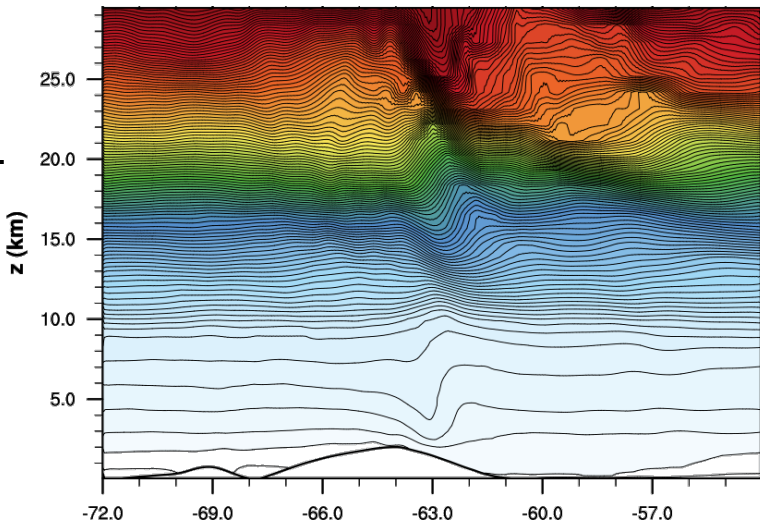
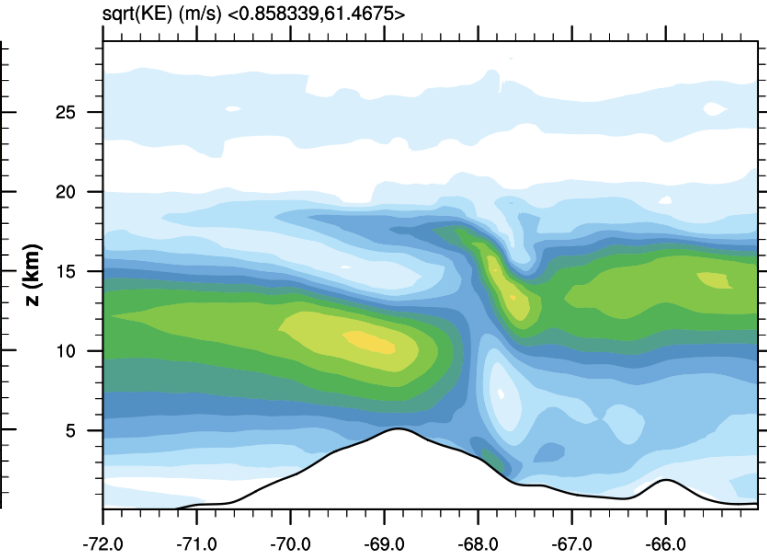
MPAS 30 h Forecast, Valid 10-29-2010 06Z, No Gravity-wave absorbing layer

Potential Temperature

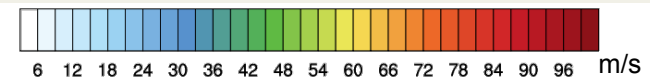
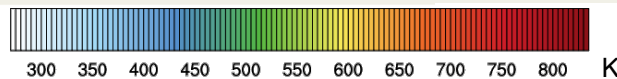
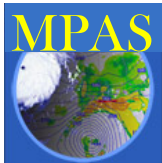
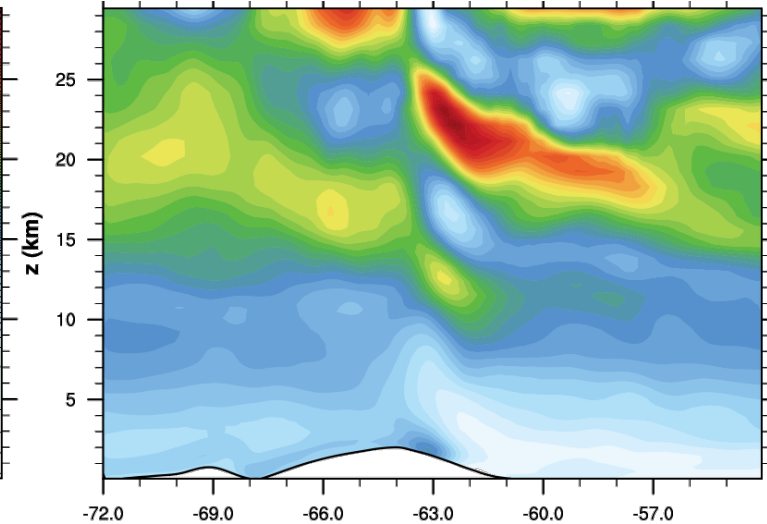


Andes Mtns
@ 28°S,
weak winds
in mid
stratosphere

Horizontal wind speed



Antarctic Pen.
@ 71° S,
strong winds
in mid
stratosphere

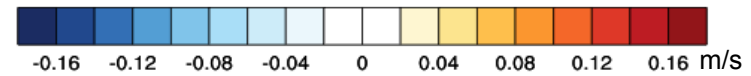
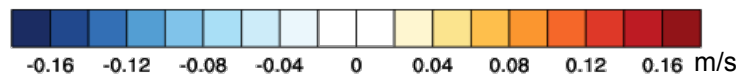
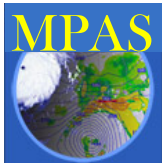
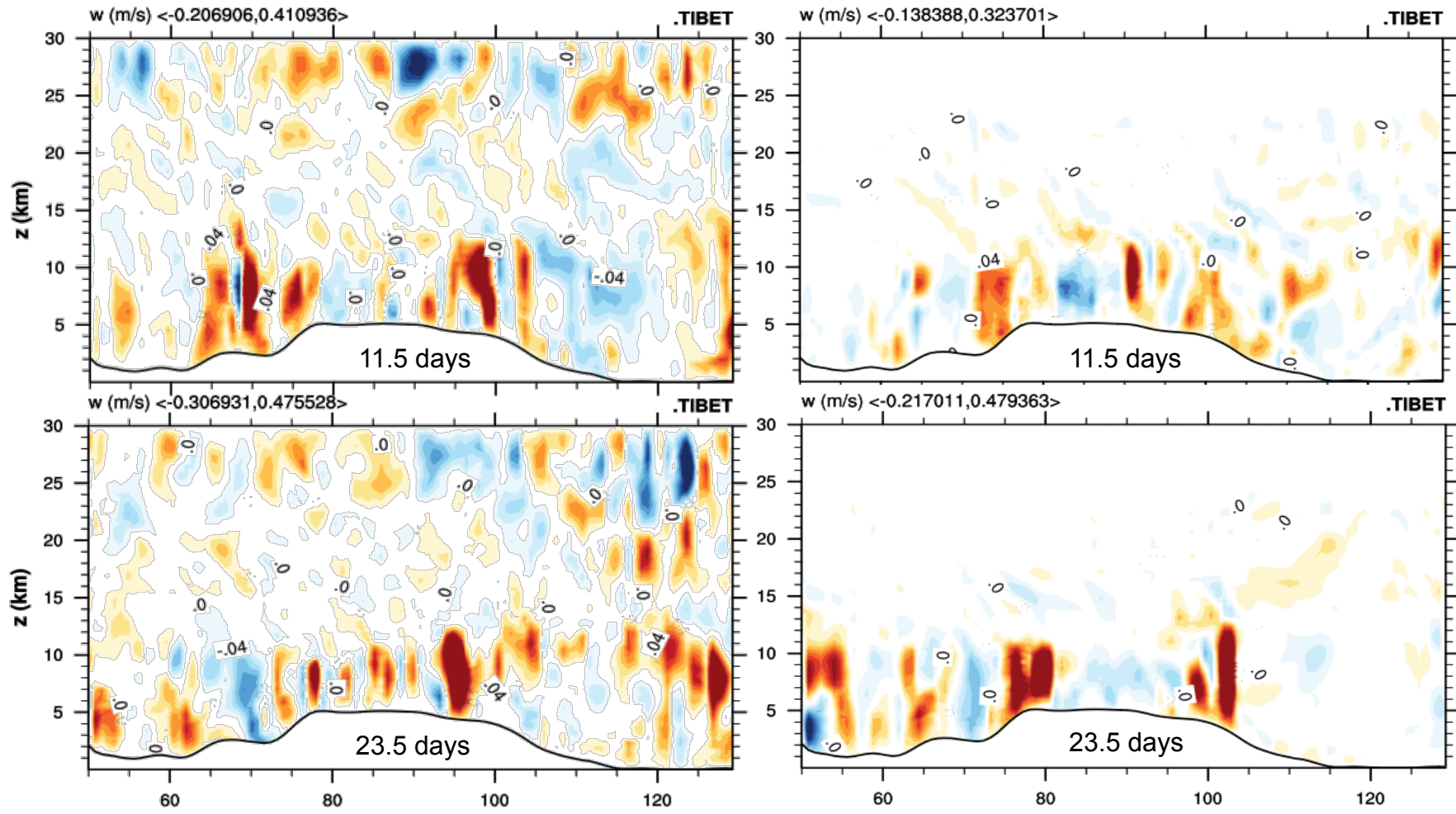


Convection over Himalayas with/without Upper Absorbing Layer

MPAS forecast on 40962 (~120 km) grid at 35° N, initialized 05-01-2005

Without Upper Absorbing Layer

With Upper Absorbing Layer



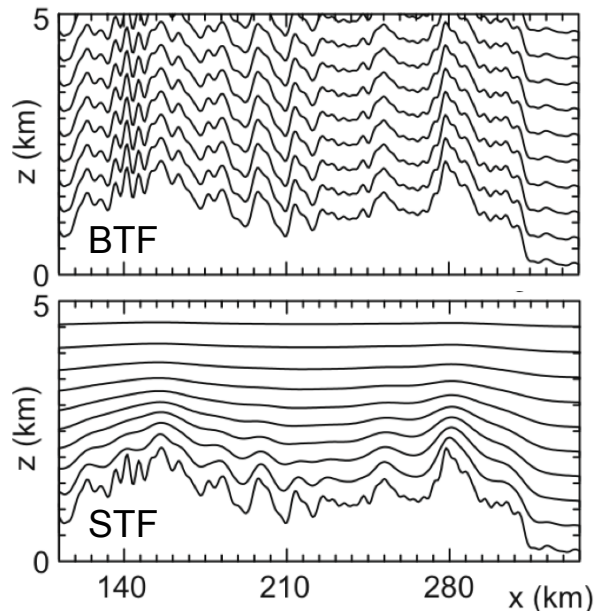
(Laura Fowler, NCAR)

Treatment of Terrain and Terrain-Following Coordinates

Specification of terrain:

- High resolution terrain data (30 arcsec) averaged over grid-cell area
- Terrain smoothing with one pass of a 4th order Laplacian

Smoothed Terrain-Following (STF) hybrid Coordinate



$$z(x, y, \zeta) = \zeta + A(\zeta)h_s(x, y, \zeta)$$

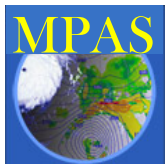
$A(\zeta)$ Controls rate at which terrain influences are attenuated with height

$h_s(x, y, \zeta)$ Terrain influence that represents increased smoothing of the actual terrain with height

Multiple passes of simple Laplacian smoother at each ζ level:

$$h_s^{(n)} = h_s^{(n-1)} + \beta(\zeta)d^2\nabla_\zeta^2 h_s^{(n-1)}$$

STF progressively smooths coordinate surfaces while transitioning to a height coordinate



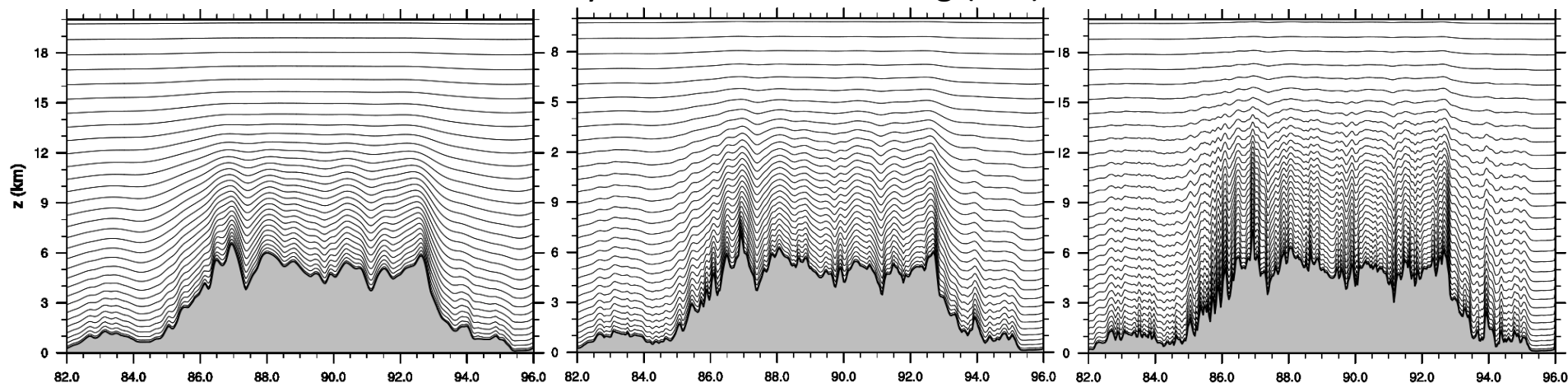
15, 7.5, & 3 km MPAS - Tibetan Plateau, 28° N

15 km grid

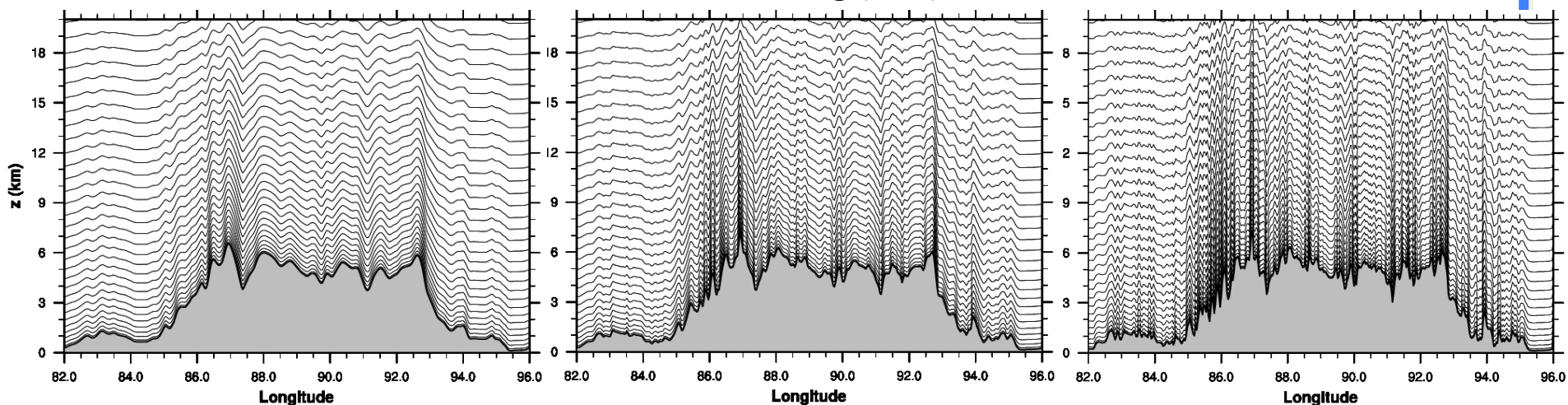
7.5 km grid

3 km grid

Smoothed hybrid terrain-following (STF) coordinate



Basic terrain-following (BTF) coordinate

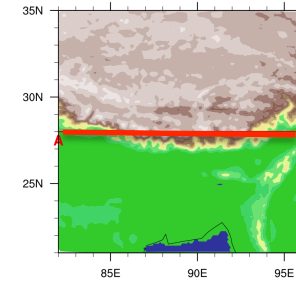


(Model top is at 30 km)

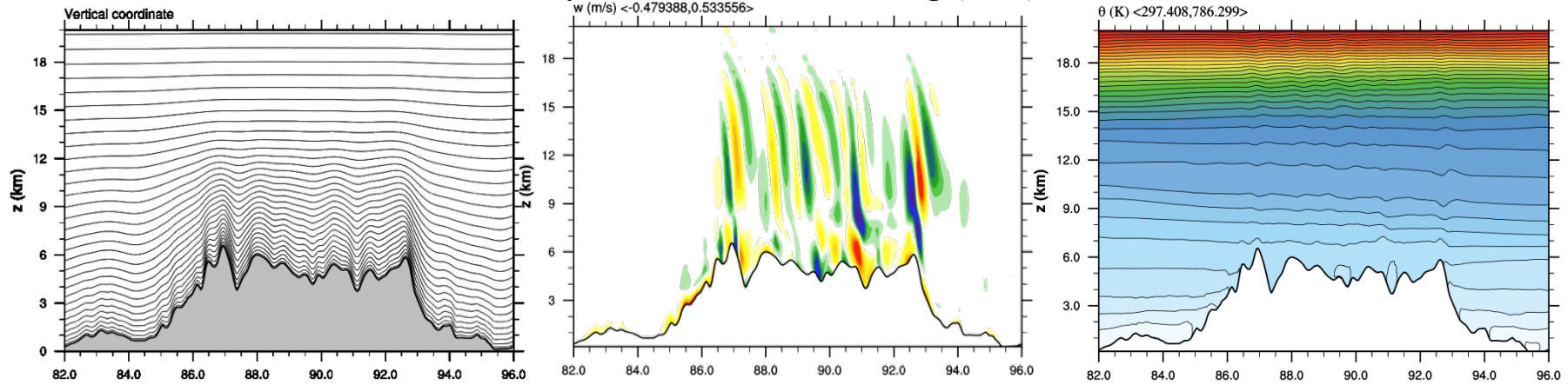
15 km MPAS Coordinate Smoothing Tibetan Plateau, 28° N

Init. 10-28-10-00Z, Valid 10-29-10-06Z

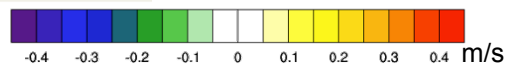
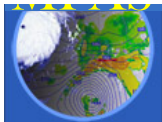
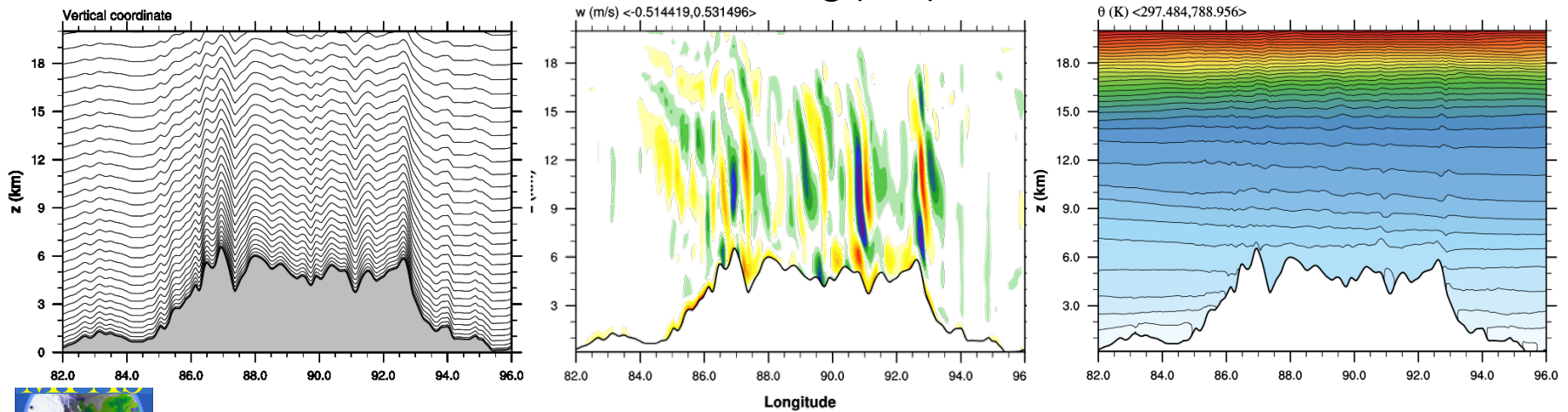
Terrain height



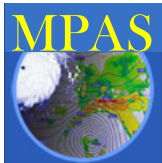
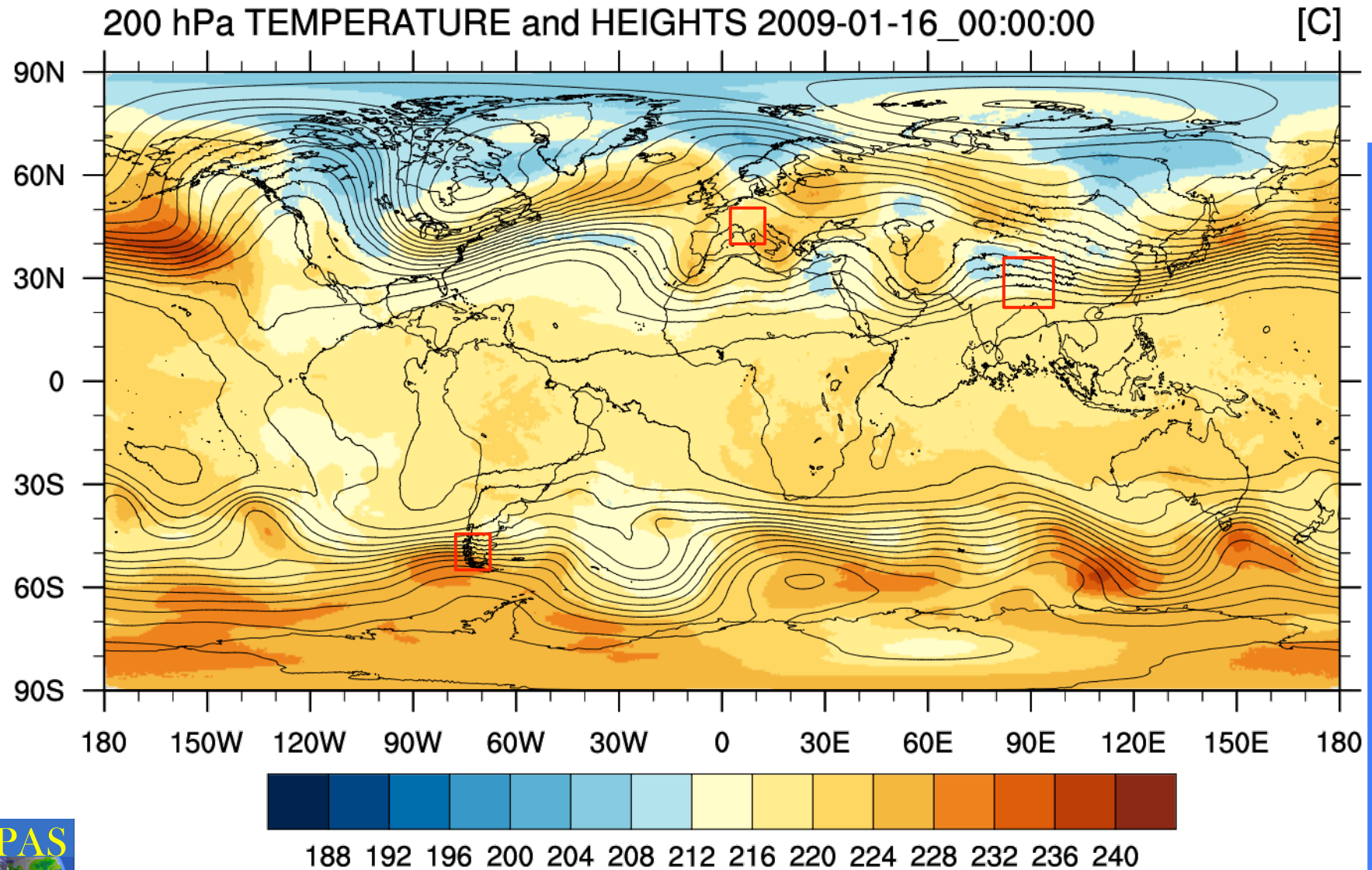
Smoothed hybrid terrain-following (STF) coordinate



Basic terrain-following (BTF) coordinate

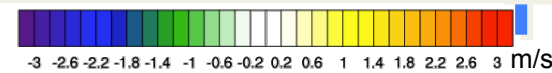
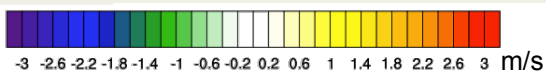
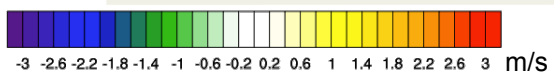
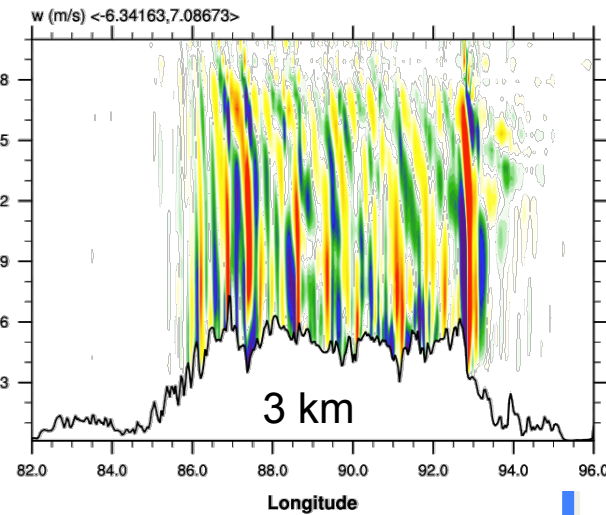
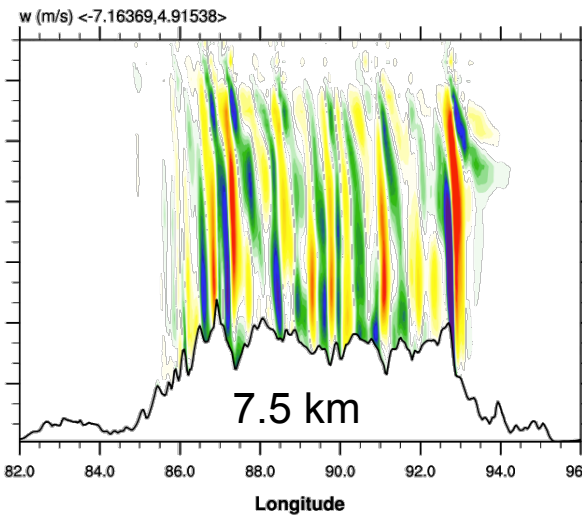
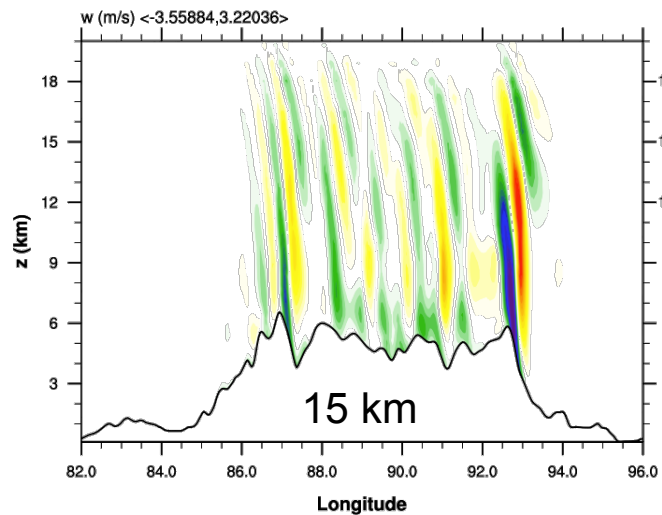
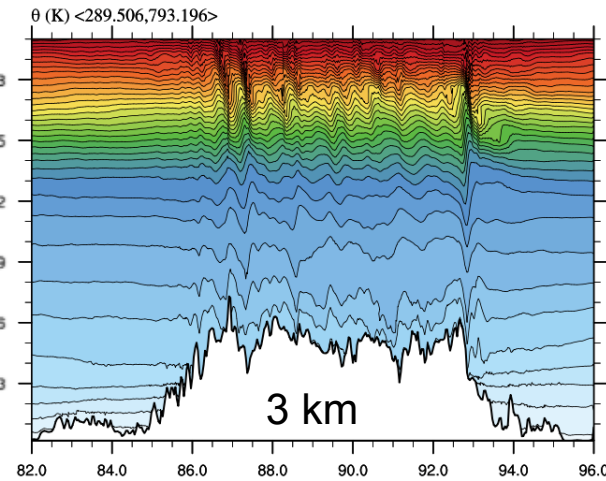
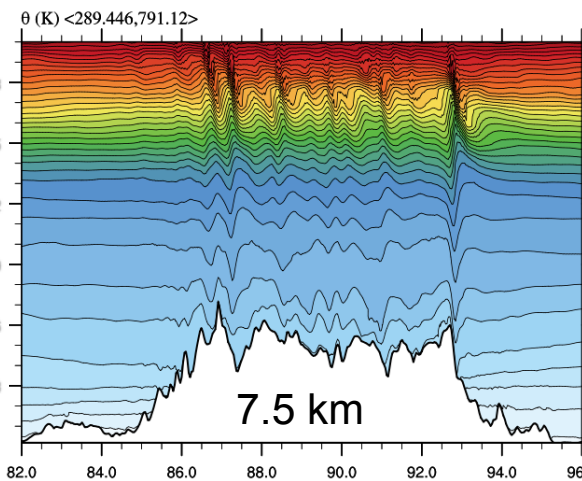
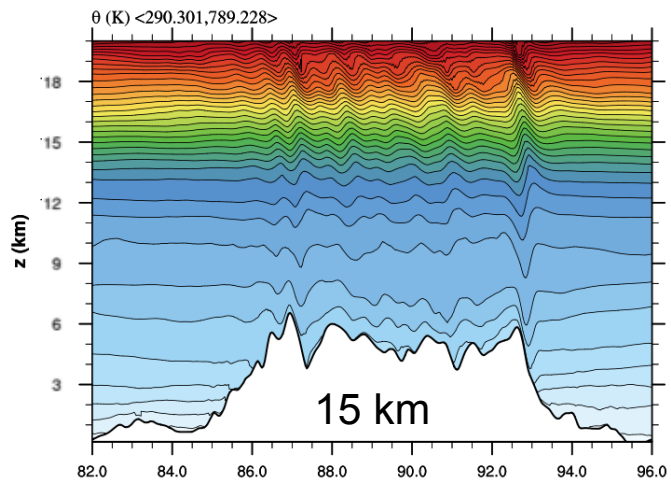
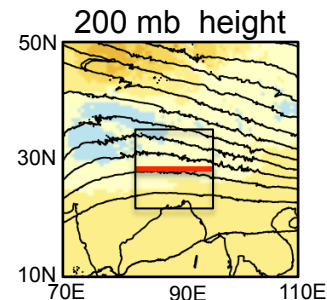
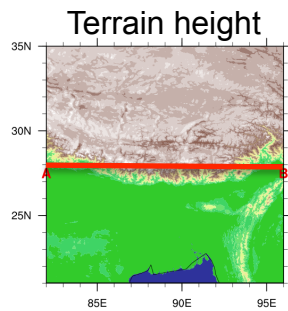


MPAS 15 January 2009 initialization



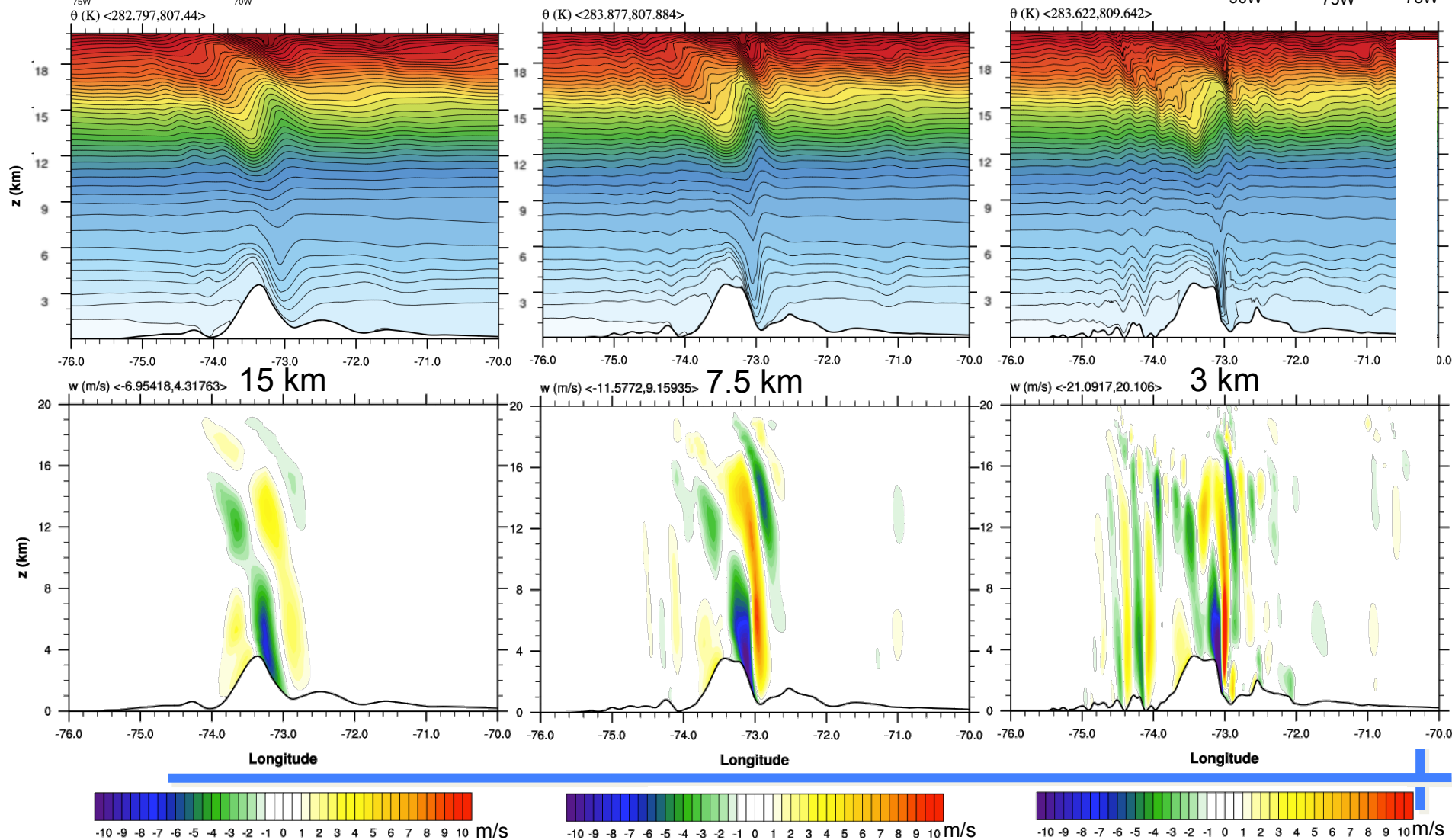
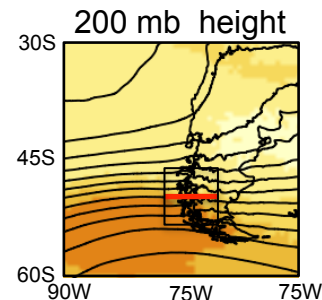
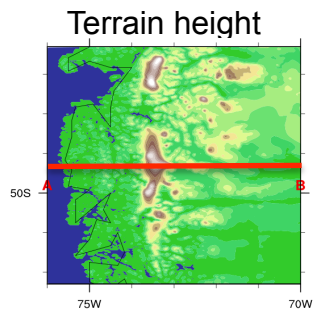
MPAS 15 January 2009 init. Tibetan Plateau at 28° N

Valid 01-16-2009 00Z



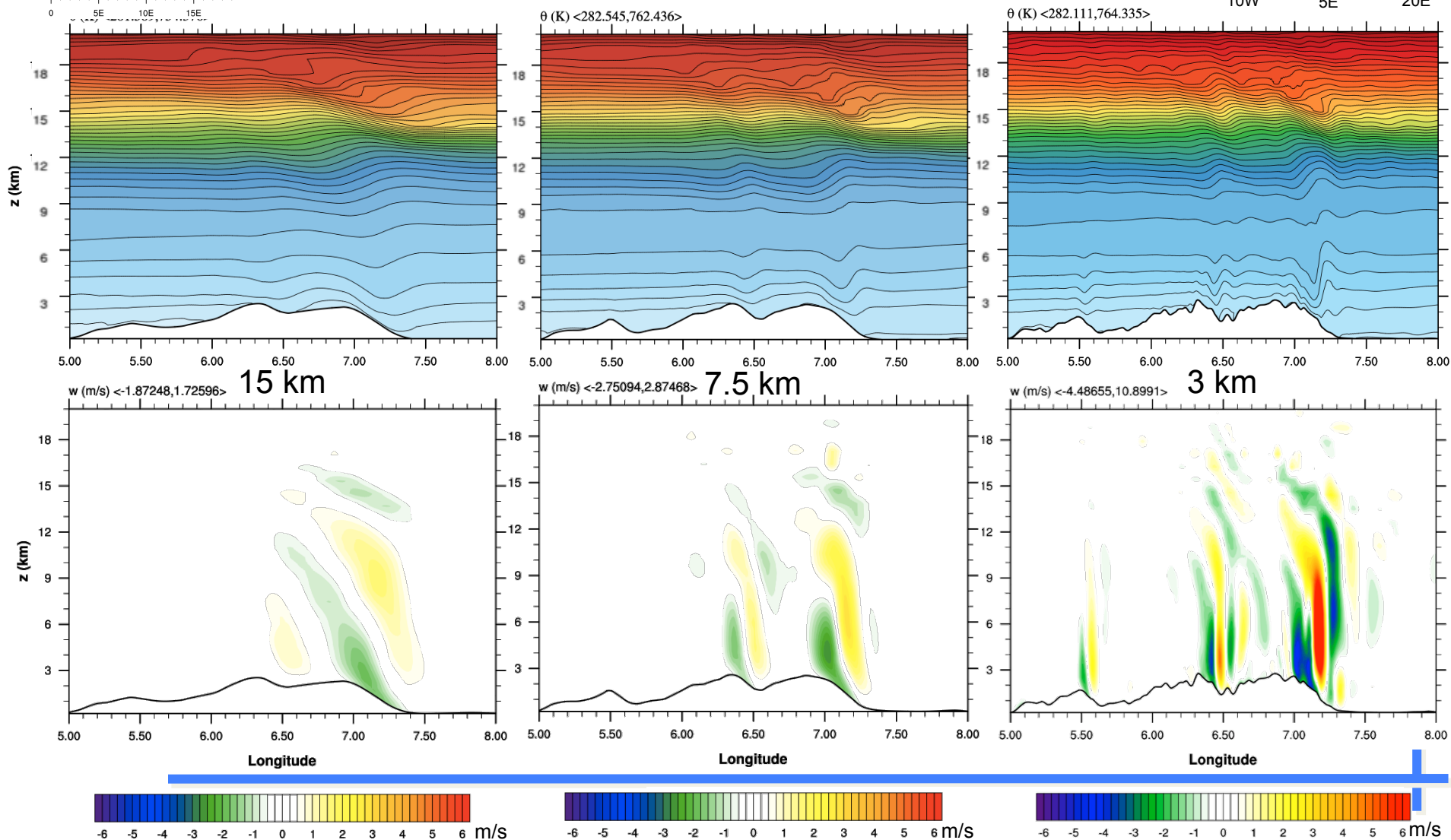
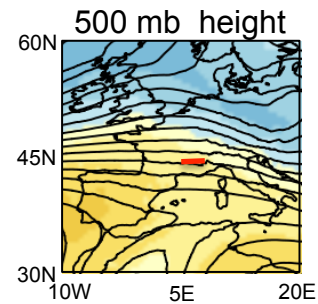
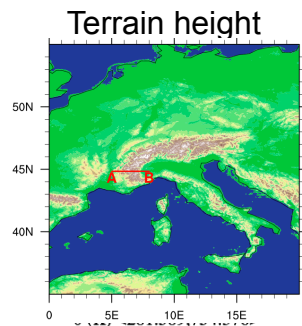
MPAS 15 January 2009 init. Southern Andes at 49.3° S

Valid 01-16-2009 00Z



MPAS 15 January 2009 init. Western Alps at 44.8° N

Valid 01-19-2009 06Z



Summary Comments

- Upper absorbing layer for vertical velocity appears to have beneficial effects at all scales tested
- Smoothed hybrid terrain-following coordinate appears to produce somewhat smoother flow fields over mountainous terrain than basic terrain-following coordinates.
- Preliminary testing has shown little sensitivity to alternative horizontal pressure gradient formulations.
- Mountain-wave structures exhibit strong dependence on horizontal resolution over the 15-3 km grid range.
 - Horizontal scales continue to decrease and vertical velocities increase with increasing resolution (not approaching convergence).
 - Increasing smaller scale structure in terrain appears key to the resolution sensitivity

